

Thermomechanical Instabilities in Metal-Free Friction Materials Using a Nonlinear Transient Simulation Approach

Kingsford Koranteng, Joseph-Shaahu Shaahu, and Yun-Bo Yi University of Denver

Citation: Koranteng, K., Shaahu, J.-S., and Yi, Y.-B., "Thermomechanical Instabilities in Metal-Free Friction Materials Using a Nonlinear Transient Simulation Approach," SAE Technical Paper 2021-01-1286, 2021, doi:10.4271/2021-01-1286.

Abstract

he invention of metal-free friction materials is gaining popularity in the manufacturing of brake pads and clutch friction discs because of the negative factors associated with metals such as copper. To gain more insight into the failure mechanism of the recent invention during brake or clutch applications, a nonlinear transient thermomechanical model is established using Finite Element Code. The model is based on a two-dimensional configuration for an investigation on the onset of TMI (Thermo-Mechanical Instability) during sliding contact in such material. The model is validated by

comparing the transient simulation results for a full-contact regime to the result from the existing eigenvalue method. A parametric study is carried out to examine how the thermal conductivities and the elastic moduli influence TMI. The simulation results show that the thermal conductivities in the transverse direction and elastic moduli in the longitudinal direction can stabilize the system. Conversely, the elastic moduli in the transverse direction and thermal conductivity in the longitudinal direction were found to enhance TMI formation. Overall, the elastic moduli and thermal conductivities in the longitudinal direction tend to play a minor role in TMI.

Introduction

hermomechanical instability, which involves the coupling between the traditional thermoelastic instability and other physical interactions such as wear, convective cooling, material nonlinearities, etc. has become an important subject to researchers and manufacturers in the automotive industry. This is because the response of a sliding system in contact interactions involves not only TEI but other distinct physical fields and properties. In clutch and brake applications, friction material properties play an excellent role in determining the onset of TMI during sliding contact. To manage TMI in clutch and brake applications, manufacturers usually employ various metal compositions such as copper to friction materials to enhance the thermal and mechanical behavior of the sliding system. The absence of metals may cause the friction material to be more susceptible to thermomechanical instability (TMI). Meanwhile, the harmful effect of metals on the environment requires manufacturers to switch to a more environmentally friendly friction material. The evolutions of metal-free friction materials require an in-depth understanding of the material response to thermomechanical distortion to prevent the formation of hotspots, wear, noise, and vibration [1]. Thermomechanical instability in clutch and brakes have long been studied using various approaches by considering the traditional TEI and different material properties. The method for determining TEI was pioneered by Burton et al [2]. Moreover, many researchers have developed different approaches to estimate the onset of TEI but rely on the condition that if the sliding speed of the

system exceeds a certain critical value, then TEI occurs. This is usually done by imposing a harmonic perturbation in the form of pressure or temperature between the sliding surface and observing the growth of the perturbation. For instance, Azarkhin and Barber [3] and Dow and Burton [4] shown that, when a small harmonic perturbation is imposed between two half-planes, the planes become unstable when the sliding speed exceeds a certain critical speed. Lee and Barber [5] extended this approach to the case of a layer finite thickness sliding between two have planes. Further, an analytical model for the symmetric and antisymmetric modes was developed by Jang and Khonsari [6] to analyze the contact between an insulator and a conductor. It was revealed that critical speed is governed by five independent dimensionless parameters. The authors also employed the condition that thermoelastic instability occurs when the sliding speed exceeds a critical value to determine the threshold of thermoelastic instability in friction pairs by considering the surface roughness effect [7].

In a thermo-mechanical analysis in brakes and clutches, the transient modal approach is usually recommended because it provides an efficient numerical algorithm for the analysis of TMI [8]. A simple approach to the transient solution of TEI was carried out by Al-Shabibi and Barber [9] using a truncated series approach (reduced-order models). Also, the fast speed expansion method could be used as carried out by Li and Barber [8]. Meanwhile, to ensure accuracy, a straightforward approach is to use a finite element discretization method. This method is preferable since it can be implemented in FEA software without the user developing any new code.

Nonetheless, there is some limitation to the use of the FEA in TEI analysis. For example, the relative motion of the sliding component implies that at least one of the components will be moving relative to the FEA reference frame. Also, the resulting convection terms in the heat conduction lead to the problem of convergence and stability [10]. An early attempt at using the numerical approach to study TEI was made by Kennedy and Ling [11]. Zagrodzki [12] used the numerical approach to investigate the transient thermomechanical phenomena for multi-disk clutch. Moreover, the non-linear transient behavior of a sliding system with TEI was studied by Zagrodzki et al. [13]. The authors investigated the migration speed generated during sliding contact. A similar study was also conducted by Al-Bahkali and Barber [10]. The authors investigated the nonlinear steady-state solution for the thermoelastic sliding system using FEA.

Existing research works on thermo-mechanical instability or the traditional thermoelastic instability are usually based on the response of friction materials whose properties are variant with respect to direction. More importantly, the approach is based on the eigenvalue approach which implies that contact must be conforming, thus no contact surface separation is allowed. Meanwhile, at elevated temperatures, two sliding surfaces in contact may experience some localized region separation due to material and geometry non-linearity. The use of the transient approach deals with the nonlinearities such as surface separation, wear effect, convective cooling, asperity contact, etc. Researchers such as Zhao et al.[14] have carried out a series of work on the influence of material properties such as thermal conductivities, elastic moduli, and thermal expansion coefficient on TEI. Meanwhile, the influence of these properties in the various directions (longitudinal, shear, and transverse directions) as in the case of the metal-free friction material was not considered. The present study considers the influence of properties in the longitudinal and transverse direction on TMI by considering the coupling effect of convection cooling and separation effect using a nonlinear transient approach. The developed model uses an iterative process until the solution converges. The iterative process required the use of Finite Element Code, FORTRAN, and MATLAB.

Metal-Free Friction Material

We used the properties of a carbon-fiber-reinforced hybrid composite friction material made of woven yarn for the simulation. This material is considered metal-free because it has no metal compositions. The mechanical stiffness matrix and thermal properties of this material are obtained using the rule of mixture by modifying the friction material presented by Biczó et al., [15] to exclude the copper component. Moreover, because the TMI model is a 2-dimensional configuration, material parameters in the x-direction (longitudinal) and y-direction (transverse) were considered as shown in Table 1.

TABLE 1 Mechanical and thermal properties of the carbon fiber-reinforced composite friction material

Thermomechanical properties of the metal-free friction material	
E ₁₁ (GP a)	11
E₂₂ (GPa)	11
G₁₂ (GPa)	7.6
V ₁₂	0.25
k ₁₁ [W/(m.K)]]	4
k₂₂ [W/(m.K)]]	4
α_{11} , α [(10 ⁻⁶ / $^{\circ}$ C)]	12
$lpha_{ t 22}$, $lpha$ $[(t 10^{-6}/\ ^{\circ}\ t C)]$	12

TMI Model Formulation

The TMI problem, involving the sliding of two discs was modeled as blocks. Boundary conditions were applied to the model to depict two small circular discs or rings. This simplified model is an accurate representation of the sliding behavior of a full brake disc or clutch because the solution is periodic in the sliding x-direction by applying cyclic symmetry boundary conditions. The period corresponds to an integer submultiple L = C/W of the circumference C of the disc, where W is the wavenumber [10]. The material properties listed in Table 1 and Table 2 represent the friction and steel disc blocks respectively. Both blocks are considered elastic and thermally conducting. Figure 1 shows the schematic of the two-disc blocks of different materials. Block 1 is the composite friction material while block 2 is the conducting steel disc. Block 1 moves in-plane with a sliding speed V with respect to block 2. Moreover, Block 1 can move in both the x and y directions while block 2 stays stationary. The two blocks have equal length L and heights of h_1 and h_2 respectively. When $y = y_1$ represent the contact interface between the two blocks. The formulation of the TMI model consist of thermal analysis and a static elastic analysis which were both carried out using Finite Element Code.

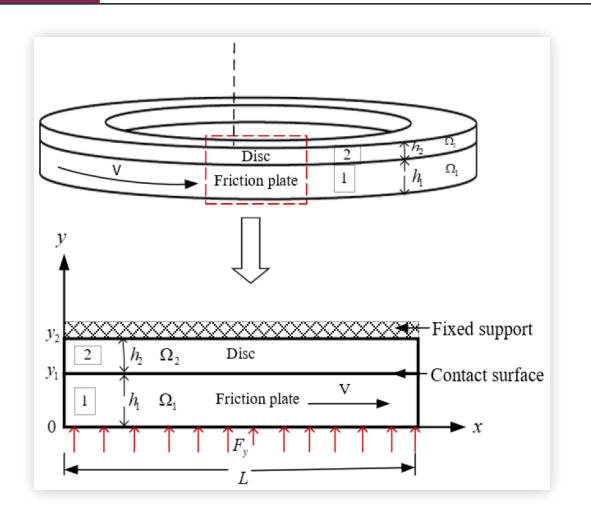
Boundary Conditions for Thermal Analysis

If the surface $y=y_1$ are in perfect contact, thus the clearance $\Delta u_{y1} = 0$, then the contact is given implicitly by the conservation of energy condition.

TABLE 2 shows the material properties of the conducting materials used in this analysis

Properties	Conducting material (Steel)
Modulus of Elasticity, E, GPa	210
Conductivity K, (W/m ° C)	57
Poisson's ratio, υ	0.4
Thermal Expansion coefficient, α , (μC^{-1})	12
Density, ρ , kg/m³	7250
Specific heat, α , (C^{-1})	460

FIGURE 1 Schematic of the sliding components



$$K_1 \frac{\partial T_1}{\partial y} \bigg|_{y=y_1} - K_2 \frac{\partial T_2}{\partial y} \bigg|_{y=y_1} = q \tag{1}$$

At initial condition, the boundary condition at the surface of the sliding component is given as:

$$T_1\big|_{\nu=\nu 1} = T_2\big|_{\nu=\nu 1} = 0$$
 (2)

Further, at x = 0 and x = L, cyclic symmetry boundary conditions are imposed on the sides of the two blocks. This is to ensure that the temperatures at the two opposite edges of each block are the same to depict the sliding behavior of a complete circular disc instead of two blocks sliding.

$$T_2\big|_{x=0} = T_2\big|_{x=L} \text{ and } T_1\big|_{x=0} = T_1\big|_{x=L}$$
 (3)

In addition, surface film conditions were defined at Ω_1 and Ω_2 as shown in <u>Fig. 1</u> with a convection coefficient of 2 W/(m²K) at an ambient temperature of 273K. This is very important to prevent heat build-up due to the absence of heat loss. In the thermal analysis, the code is written based on the boundary conditions to compute the temperature change during contact interaction.

Boundary Conditions for the Elastic Analysis

The general static, elastic contact in Finite Element Code was used to compute the resulting pressures during the contact of the two sliding blocks. The following boundary conditions were considered:

With reference to **Fig.1**, at the edges y = 0 and $y = y_2$, the following boundary conditions were imposed.

$$\left(u_{y}\right)_{1}\Big|_{y=0} = 0 \text{ and } \left(u_{y}\right)_{2}\Big|_{y=0} = \text{Constant}$$
 (4)

Where U_y denotes the displacement of the nodes in the y-direction.

Also, an external force F_y was applied at this boundary condition to serve as a control in the y-direction by keeping the two blocks in contact without a sudden separation. Moreover, at the side edges of the blocks where x = 0 and x = L, cyclic symmetry boundary conditions were defined for the displacement of the nodes. This was to depict the behavior of

the sliding of two complete circular discs instead of the sliding of two blocks.

$$(u_x)_{1,2}\Big|_{x=0} = (u_x)_{1,2}\Big|_{x=1}$$
 and $(u_y)_{1,2}\Big|_{x=0} = (u_y)_{1,2}\Big|_{x=1}$ (5)

Further, at y=2, block 2 was constrained to prevent it from moving further away in the positive y-direction due to the externally applied force F_v .

The Solution to the TMI Procedure

We start by defining a small sinusoidal perturbation on the mean contact pressure. The perturbation could be any noise imposed on the mean pressure. This noise can always be decomposed into Fourier series where each term is a sinusoidal wave. Therefore, we can directly add the sinusoidal wave to the mean pressure as a form of noise. The mean pressure and the harmonic pressure perturbation are imposed on the system and is expressed as:

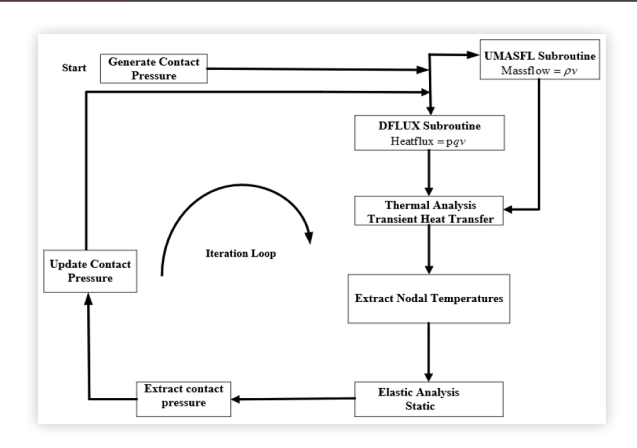
$$p(x,t) = P_m + A\sin(\omega x + \phi) \tag{6}$$

Where P_m is the mean pressure and the remaining term represents the harmonic pressure perturbation; A is the amplitude of the perturbation; x is the distance (m); \emptyset is the phase angle, ω is the angular velocity (rad/s).

The frictional heat generated is computed by using the variable contact pressure obtained from Equation 6. Similarly, the mass flow is defined in terms of the density, ρ of the composite friction material, and the sliding velocity, v. A transient heat analysis is carried out using Finite Element Code coupled with FORTRAN and MATLAB and the resulting nodal temperatures are extracted from the contacting interface at y=y1. The extracted nodal temperatures are fed into the elastic part of the analysis.

In the thermoelastic analysis, the resulting pressure distribution is extracted from the contact interface and the new nodal contact pressure is used to compute the heat flux for the next transient heat analysis. The process is repeated using an iteration scheme established using MATLAB until the solution converges and the resulting temperature and pressure growth are observed. Figure 2 illustrates the entire iterative process discussed.

FIGURE 2 Block diagram of the solution procedure



It is noteworthy that if the sliding speed is below the critical speed, the expected temperature decays at each iteration and converges to uniform contact pressure. Meanwhile, when the sliding speed, V is above the critical speed V_C , the imposed pressure perturbation grows and eventually reaches a condition where some nodes separate.

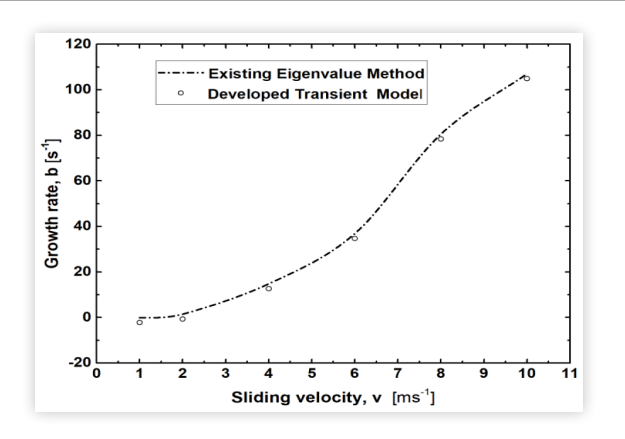
Comparison with Eigenvalue Approach

The developed TMI model was validated by comparing the result of a full-contact regime analysis (contact without separation) to that of existing eigenvalue approach using HOTSPOTTER. The model was validated using a full-contact regime because Hotspotter is based on the eigen value approach and is not able to handle geometry and material non-linearity. The material properties listed in Table 1 & 2 were used. Moreover, HOTSPOTTER only permits the entry of isotropic material property for the thermal conductivity, hence we computed the average thermal conductivity in the longitudinal and transverse direction and used it in both models. We also neglected surface film conditions in both. Figure 3 presents the comparison of the growth-rate against velocity for the two models. We can see that the results from the developed transient model agree extremely well with the results from HOTSPOTTER for a full-contact analysis. The accuracy of the present model provides confidence in the output results from the simulations carried out in this work.

TMI with Separation Effect

In TMI analysis, it is always essential to consider the separation effect since above certain critical speed, the steady-state problem may involve regions of separation and the problem may become non-linear. For separation to occur, the imposed harmonic perturbation increases at each iteration, creating a condition where some contact nodes start to separate. This is accompanied by a rapid contraction of the contact area and a corresponding increase in the maximum contact pressure. Thus, illustrating the nature of the hot spot formed on the discs. Further, the amplitude of the perturbation will continue to increase at the contact surface as more nodes separate with

FIGURE 3 Growth rate vs. sliding velocity as determined by existing eigenvalue and the simulated model



further iterations until the solution converges. The non-uniform contact pressure distribution on the contact surface leads to the non-uniform distribution of temperature which causes hotspot, judder, and thermal buckling as observed on brake and clutch discs [16, 17, 18].

Results

Thermal Conductivity

Thermal conductivity forms an important factor relating to system stability as reported by Zhao et al. [14]. The critical speed of friction materials has been found to increase as thermal conductivity is increased. This shows how important the parameters play in ensuring system stability. This work further investigates how the thermal conductivity in the longitudinal direction and transverse direction affect the stability of the sliding system using a transient approach. We carried out the simulation for a time period of t = 0.8s under a sliding velocity of v = 3.0m/s

Longitudinal Direction (K₁₁)

We start by keeping all parameters listed in <u>Table 2</u> constant, except for the thermal conductivity in the longitudinal direction ($K_{11} = 1, 2, 3, 4 \ W/m \,^{\circ} C$). Fig. 4 show the resulting contact pressure distribution by varying the thermal conductivity K_{11} . Increasing the thermal conductivity K_{11} exhibited no significant effect on the system instability. Meanwhile, when the thermal conductivity $K_{11} = 4 W/m$ ° C is equal to the constant value of thermal conductivity $K_{22} = 4 W/m$ ° C (thickness direction), $P(x, t)/P_m$ decreases from 11.14 to 10.79. A further study showed that the contact pressure increases again when K_{11} is greater than the constant value of K_{22} . This could be explained by observing the temperature distribution profile in Fig 5. When K_{11} was equal to K_{22} , there is a slight drop in temperature. Hence, the corresponding contact pressure. Moreover, further studies need to be carried out to determine this phenomenon.

FIGURE 4 Contact pressure distribution for thermal conductivity in the longitudinal direction

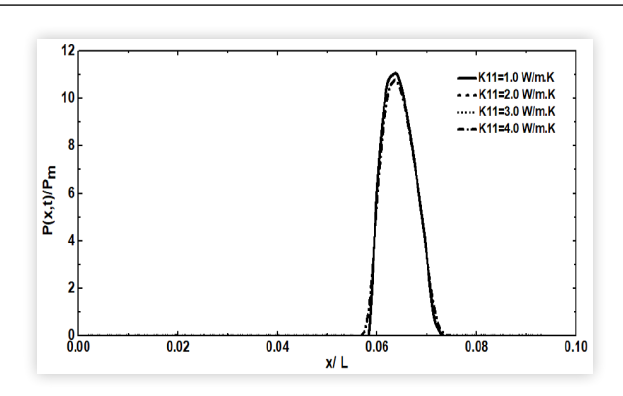
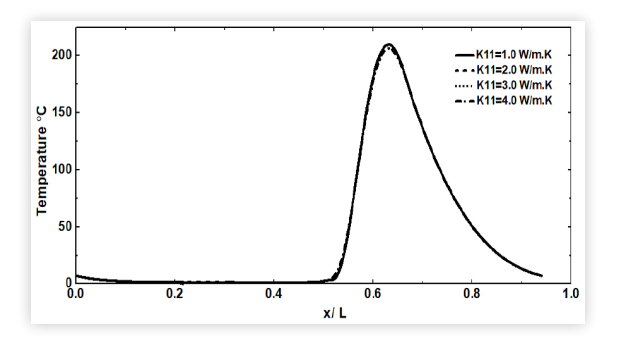


FIGURE 5 Temperature distribution along the contact surface for thermal conductivity



Transverse Direction/ Thickness Direction (K₂₂)

The thermal conductivity in the transverse direction was varied ($K_{22} = 1, 2, 3, 4 W/m \circ C$) while keeping all other material properties constant. Figure 6 show the resulting contact pressure distribution. The effect of contact pressure on the system stability was significant. Increasing K_{22} stabilizes the system. The pressure perturbation is observed to decays significantly as K_{22} is increased. For example when $K_{22} = 1.0 W/m$ ° C, separation occurred at certain regions accompanied by a rapid contraction of the contact area from x/L = 0.52 to 0.68. The maximum value $(P(x, t)/P_m)$ exhibited is 10.96. Further increasing the $K_{22} = 2$, 3, 4 W/m ° C caused certain regions to have more contact interaction leading to the evolution of new local maximum pressures. This is because the uniformity of the contact pressure is enhanced leading to a gradual improvement in the temperature distribution on the contact surface as seen in Fig. 7.

Meanwhile, when thermal conductivity is increased gradually to $K_{22}=4.0W/m$ ° C, the temperature profile assumes a more uniform profile. It starts at T=88.4 ° $\mathbb C$ and decrease slowly to T=13 ° $\mathbb C$, at x/L=0.37. It then rises slowly to a local maximum value of T=82.3 ° $\mathbb C$ at x/L=0.49. The maximum pressure was observed to T=85 ° $\mathbb C$, at x/L=0.94. Therefore, it can be said that, increasing K_{22} improves the uniformity of temperature distribution and hence, stabilizing the system.

FIGURE 6 Contact pressure distribution with separation effect

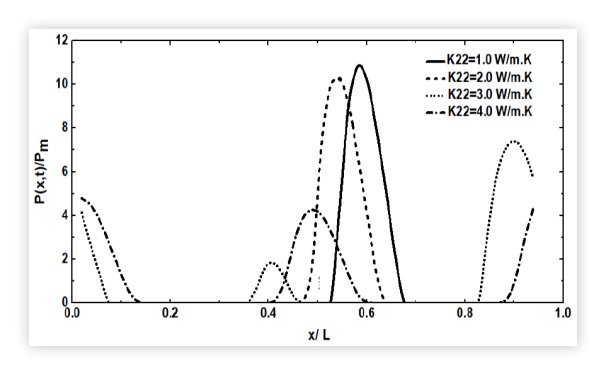
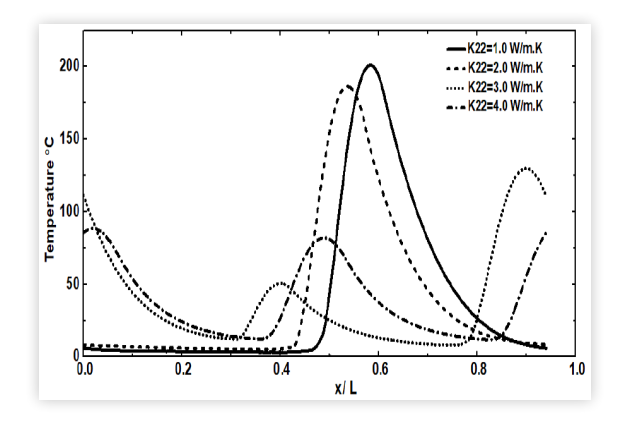


FIGURE 7 Temperature distribution for thermal conductivity in the transverse direction



Elastic Modulus

Literature works have shown that materials with high elastic modulus encourage the formations of hot spots and the subsequent result is system instability. Moreover, works on the elasticity of materials whose properties are not invariant with respect to direction and how they contribute to TMI formation are lacking in research. We investigated the unstable behavior of the friction material caused by the elastic modulus in the longitudinal E_{11} and thickness direction E_{22} .

Longitudinal Direction (E₁₁)

The elastic modulus in the longitudinal direction was varied $(E_{11} = 9,10,11,12GPa)$ while keeping all other parameters constant. The resulting contact pressure distributions by varying this parameter are shown in <u>Fig. 8</u>. It was revealed that contact pressure decreases as elastic modulus E_{11} is increased.

Thus, instability decreases slightly as E_{11} is increasing. It can be deduced from this behavior E_{11} in the longitudinal direction can stabilize the system. The corresponding temperature distributions (Fig. 9) show that there is a slight reduction in the maximum temperature from $T=211.25\,^{\circ}$ C to $T=206\,^{\circ}$ C as E_{11} is increased from $E_{11}=9$ GPa to

FIGURE 8 Contact pressure distribution for elastic modulus in the longitudinal direction

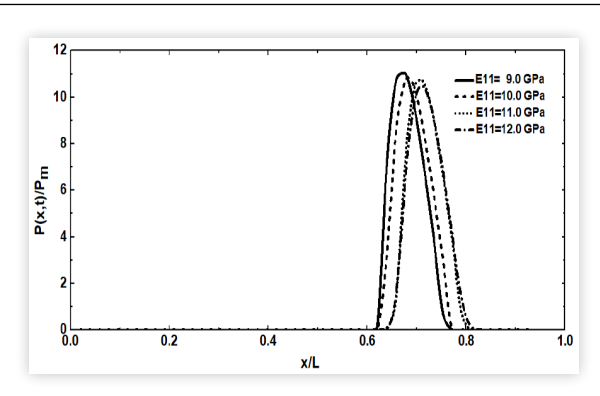
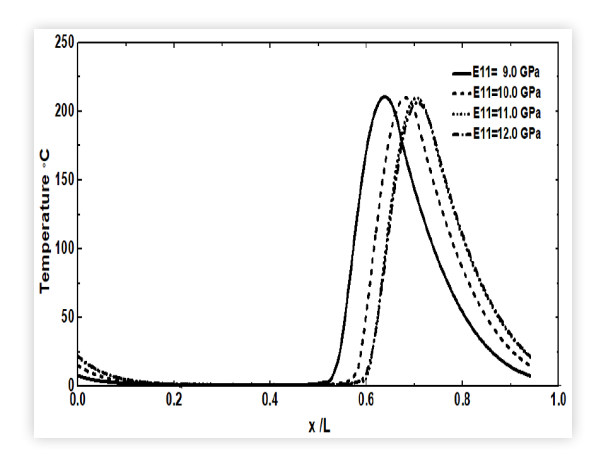


FIGURE 9 Temperature distribution for elastic modulus in the longitudinal direction



 $E_{11}=12$ GPa. Further, the direction of the perturbation is influenced strongly by E_{11} . We can also deduce that the uniformity of temperature is improved slightly by increasing E_{11} . For example, near the end of the contact pressure distribution profile at x/L=0.94, temperatures were observed to be T=7.98 ° $\mathbb C$, 14.36 ° $\mathbb C$, 21.9 ° $\mathbb C$, 22.1 ° $\mathbb C$ for $E_{11}=9,10,11$ and 12 GPa respectively.

Transverse Direction (E22)

Figure 10 shows the evolution of contact pressure distribution by varying the young modulus in the thickness direction $E_{22} = 9,10,11,12$ GPa. The results show that elastic modulus in the thickness direction significantly promotes TMI formation. Increasing E_{22} caused the contact pressure to grow gradually. This can be attributed to the fact that the thickness direction of the material dominates which leads to higher contact pressure and thus a higher friction heat generation. This causes the growth rate to increase as the critical speed is decreased. Thus, making the friction material more susceptible to TMI as the temperature is seen to increase as elastic modulus E_{22} is increased (Fig.11).

FIGURE 10 Contact pressure distribution with separation effect

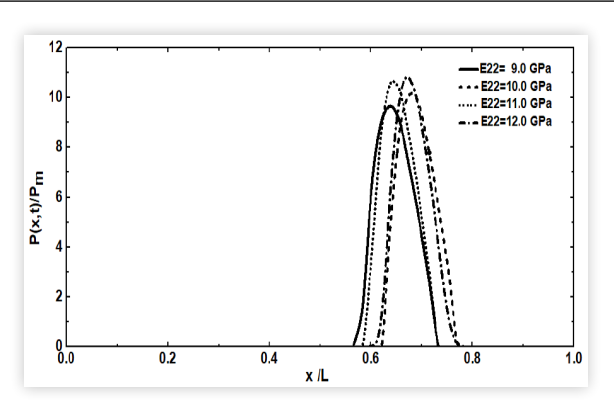
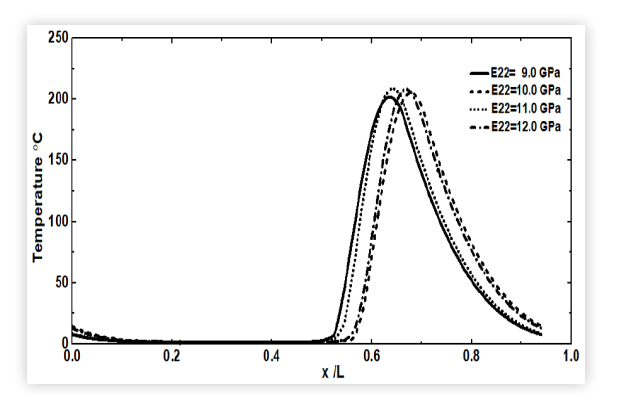


FIGURE 11 Temperature distribution for elastic modulus in the longitudinal direction



Conclusion

A two-dimensional thermomechanical model is developed to investigate the effect of elastic modulus and thermal conductivity in the longitudinal and thickness direction of a metal-free friction material while considering contact with separation effect. The model is validated by comparing with the existing eigenvalue approach by considering full contact analysis. Increasing elastic modulus E_{11} and thermal conductivity K_{22} were found to discourage TMI formation. Thus, a friction material with higher elastic modulus in the sliding direction and thermal conductivity in the thickness direction enhances sliding stability. Conversely, increasing thermal conductivity K_{11} and Elastic modulus E_{22} were found to make the friction material more susceptible to TMI formation. This implies that friction materials with a higher thermal conductivity in the sliding direction and elastic modulus in the thickness direction promote sliding instability leading to hot spot formation, judder, vibration, and noise. Nonetheless, when the value of K_{11} was approximately equal to K_{22} , slight stability was observed.

Acknowledgment

Support for this work, provided by the National Science Foundation under Contract (No. 1928876), is gratefully acknowledged.

References

- Kao, T.K., Richmond, J.W., and Douarre, A., "Brake Disc Hot Spotting and Thermal Judder: An Experimental and Finite Element Study," *International Journal of Vehicle Design* 23, no. 3 (2000): 276-296.
- Burton, R.A., Nerlikar, V., and Kilaparti, S.R., "Thermoplastic Instability in a Seal-Like Configuration," 12, 1973.
- 3. Azarkhin, A. and Barber, J.R., "Thermoplastic Instability for the Transient Contact Problem of Two Sliding Half-Planes," *Journal of Applied Mechanics* 53, no. 3 (1986): 565-572, doi:10.1115/1.3171812.

- 4. Dow, T.A. and Burton, R.A., "Thermoelastic Instability of Sliding Contact in the Absence of Wear," *Wear* 19, no. 3 (1972): 315-328, doi:10.1016/0043-1648(72)90123-8.
- Lee, K. and Barber, J.R., "Frictionally Excited Thermoelastic Instability in Automotive Disk Brakes," *Journal of Tribology* 115, no. 4 (1993): 607-614, doi:10.1115/1.2921683.
- Jang, J.Y. and Khonsari, M.M., "A Generalized Thermoelastic Instability Analysis," *Proceedings: Mathematical, Physical* and Engineering Sciences 459, no. 2030 (2003): 309-329.
- 7. Jang, J.Y. and Khonsari, M.M., "Thermoelastic Instability Including Surface Roughness Effects," *Journal of Tribology* 121, no. 4 (1999): 648-654, doi:10.1115/1.2834118.
- 8. Li, J. and Barber, J.R., "Solution of Transient Thermoelastic Contact Problems by the Fast Speed Expansion Method," *Wear* 265, no. 3-4 (2008): 402-410, doi:10.1016/j. wear.2007.11.010.
- 9. Al-Shabibi, A.M. and Barber, J.R., "Transient Solution of a Thermoelastic Instability Problem using a Reduced Order Model," *International Journal of Mechanical Sciences* 44, no. 3 (2002): 451-464, doi:10.1016/S0020-7403(01)00110-2.
- Al-Bahkali, E.A. and Barber, J.R., "Nonlinear Steady State Solution for a Thermoelastic Sliding System Using Finite Element Method," *Journal of Thermal Stresses* 29, no. 2 (2006): 153-168, doi:10.1080/01495730500257466.
- Kennedy, F.E. Jr. and Ling, F.F., "Closure to 'Discussions of "A Thermal, Thermoelastic, and Wear Simulation of a High-Energy Sliding Contact Problem" (1974, ASME J. Lubr. Technol., 96, pp. 505-506)," *Journal of Lubrication* Technology 96, no. 3 (1974): 507-507, doi:10.1115/1.3452029.
- 12. Zagrodzki, P., "Analysis of Thermomechanical Phenomena in Multidisc Clutches and Brakes," *Wear* 140, no. 2 (1990): 291-308, doi:10.1016/0043-1648(90)90091-N.
- 13. Zagrodzki, P., Lam, K.B., Al Bahkali, E., and Barber, J.R., "Nonlinear Transient Behavior of a Sliding System with Frictionally Excited Thermoelastic Instability," *Journal of Tribology* 123, no. 4 (2001): 699-708, doi:10.1115/1.1353180.
- Zhao, J., Yi, Y.-B., and Li, H., "Effects of Frictional Material Properties on Thermoelastic Instability Deformation

- Modes," *Proceedings of the Institution of Mechanical Engineers, Part J: Journal of Engineering Tribology* 229, no. 10 (2015): 1239-1246, doi:10.1177/1350650115576783.
- Biczó, R., Kalácska, G., and Mankovits, T.,
 "Micromechanical Model and Thermal Properties of Dry-Friction Hybrid Polymer Composite Clutch Facings," *Materials* 13, no. 20 (2020): 4508, doi:10.3390/ ma13204508.
- Koranteng, K., Shaahu, J.-S., Chengnan, M., Li, H. et al., "The Performance of Cu-based Friction Material in Dry Clutch Engagement," Proceedings of the Institution of Mechanical Engineers, Part J: Journal of Engineering Tribology 135065012094428 (2020), doi:10.1177/1350650120944281.
- 17. Koranteng, K., Shaahu, J., and Yun-Bo, Y., "Transient Heat Transfer Simulation and Buckling Analysis of Disc Brakes in In-Wheel Motor Driven Vehicles," 2020.
- 18. Shaahu, J., Koranteng, K., and Yi, Y.-B., "A Coupling Analysis of Thermal Buckling and Vibration in Disc Brakes," 2020.

Contact Information

Kingsford Koranteng

PhD student Mechanical & Materials Engineering University of Denver 2155 E Wesley Ave Denver, CO 80208 Kingsford.Koranteng@du.edu

Yun-Bo Yi, Ph.D.

Professor
Mechanical & Materials Engineering
University of Denver
2155 E Wesley Ave
Denver, CO 80208
Yun-Bo.Yi@du.edu
Phone: 303-871-2228

^{© 2021} SAE International. All rights reserved. No part of this publication may be reproduced, stored in a retrieval system, or transmitted, in any form or by any means, electronic, mechanical, photocopying, recording, or otherwise, without the prior written permission of SAE International.